

Article

Demand Response Using Disturbance Estimation-Based Kalman Filtering for the Frequency Control

Xuehua Wu ¹, Qianqian Qian ² and Yuqing Bao ^{2,*} 

¹ School of Electrical Engineering, Nanjing Vocational University of Industry Technology, Nanjing 210023, China

² School of Electrical Engineering and Automation, Nanjing Normal University, Nanjing 210023, China

* Correspondence: baoyuqing@njnu.edu.cn

Abstract: Demand response (DR) has a great potential for stabilizing the frequency of power systems. However, the performance is limited by the accuracy of the frequency detection, which is affected by measurement disturbances. To overcome this problem, this paper proposes a disturbance estimation-based Kalman filtering method, which is utilized for the frequency control. By using the rate of change of frequency (RoCoF), the Kalman filtering method can estimate the state of the ON/OFF loads well. In this way, the influence of detection error can be reduced, and the DR performance can be improved. Test results show that the proposed disturbance estimation-based Kalman filtering method has a higher accuracy of frequency detection than existing methods (such as the low-pass filter method) and therefore improves the frequency control performance of DR.

Keywords: demand response; disturbance estimation; Kalman filtering; frequency control



Citation: Wu, X.; Qian, Q.; Bao, Y. Demand Response Using Disturbance Estimation-Based Kalman Filtering for the Frequency Control. *Energies* **2022**, *15*, 9377. <https://doi.org/10.3390/en15249377>

Academic Editor: Gianfranco Chicco

Received: 26 October 2022

Accepted: 6 December 2022

Published: 11 December 2022

Publisher's Note: MDPI stays neutral with regard to jurisdictional claims in published maps and institutional affiliations.



Copyright: © 2022 by the authors. Licensee MDPI, Basel, Switzerland. This article is an open access article distributed under the terms and conditions of the Creative Commons Attribution (CC BY) license (<https://creativecommons.org/licenses/by/4.0/>).

1. Introduction

The penetration of renewable energy sources is increasing nowadays, and the stability of the power system is therefore threatened [1,2]. One of the stability problems is the frequency stability, which is affected by the imbalance of active power. With the help of advanced measurement and communication technology, the demand-side appliances, e.g., air conditioners, water heaters, household refrigerators, etc., can be controlled to support not only load profiling [3], but also frequency control [4].

DR approaches are widely reported in existing research works. In Reference [4], the DR approach was considered to modify the conventional frequency response model. In Reference [5], priority management of demand-side resources was utilized to minimize the inequality between generation and demand. It is shown that DR can make a significant and reliable contribution to the primary frequency response in a manner similar to the generators [6]. Household refrigerators, air conditioners, and water heaters are familiar demand-side resources. In Reference [7], household refrigerators were combined with the flywheel energy storage system (FESS) to participate in frequency control with low consumption. In Reference [8], the characteristic of the power consumption of air conditioners was analyzed in the perspective of the DR. In Reference [9], the hybrid hierarchical control framework was proposed for ON/OFF appliances. In Reference [10], a DR operation framework was proposed for the local management of customers to participate in the electricity market. In Reference [11], dynamic interactions between local energy systems in terms of the electricity and gas networks were investigated, and a novel MT model was proposed to capture the nonlinear interactions. In Reference [12], a demand-side response method based on binomial distribution was proposed, and the individual differences in the demand-side responses were solved to improve consumer satisfaction.

Considering the influence of measurement noise in DR, the Kalman filtering method was adopted to improve the performance in the detection of the system frequency. Compared with traditional low-pass filtering methods, the Kalman filtering method is good at

dealing with process and measurement noise. The extended complex Kalman filter was proposed to estimate the frequency of the power system [13,14]. The distributed Kalman filtering scheme was proposed in the frequency estimation of the power system [15]. In Reference [16], the Kalman filtering method was adopted to estimate the state of thermostatically controlled loads, including air conditioners and refrigerators. In Reference [17], the Kalman filtering method was utilized in the frequency control based on the frequency response model, where the accuracy of the frequency estimation is improved.

Notwithstanding the contributions of the existing work, the accurate measurement of the system frequency is still challenging, which is reflected by the following two aspects:

- Although the Kalman filtering method [10–14] is good at dealing with process noise and measurement noise, it cannot cope with large disturbances, e.g., generation unit outages.
- The information of large disturbances cannot be taken as the input of the Kalman filter as such information is accidental and is not directly available.

Estimating the disturbance mixed in the noise can improve the performance of Kalman filtering-based frequency estimation and therefore contribute to the frequency control. In this paper, DR using disturbance estimation-based Kalman filtering is proposed in the frequency control. The contributions of this paper are as follows:

- The frequency response model is used to develop the Kalman filter.
- The disturbance estimation-based Kalman filtering approach is adopted in the frequency detection. The disturbance is estimated through the RoCoF.
- The hybrid hierarchical DR control strategy is adapted to the disturbance estimation-based Kalman filtering.

The remainder of this paper is organized as follows. The frequency response model and the hybrid hierarchical DR control strategy are introduced in Section 2. Section 3 presents the algorithm to estimate the system disturbance and applies the disturbance estimation-based Kalman filtering to the frequency control. Section 4 demonstrates the test results for the proposed method validation. Section 5 provides the conclusion of this paper.

2. Model Development

2.1. Frequency Response Model

The frequency response model of the power system with DR is shown in Figure 1. The definitions of the parameters are as follows:

P_{sp} is the incremental power setpoint calculated by the secondary frequency control.

ΔY is the gate position deviation.

ΔP_r and ΔP_m are the thermal power deviation of the reheated turbines and the turbine mechanical power deviation, respectively.

P_{DR} is the amount of change in the loads based on the frequency deviation.

ΔP_d is the power of disturbance (for a sudden increase in load $\Delta P_d > 0$, for a sudden increase in generation $\Delta P_d < 0$).

K_i is the integral gain of the secondary frequency control.

R is the speed droop parameter.

T_g and T_r are the speed governor time constant and the reheat time constant, respectively.

F_{HP} is the fraction of total power generated by the high-pressure turbine.

T_t is the turbine time constant.

H and D are the inertia constant and the system load damping factor, respectively.

s is the Laplace operator.

Δf is the frequency deviation.

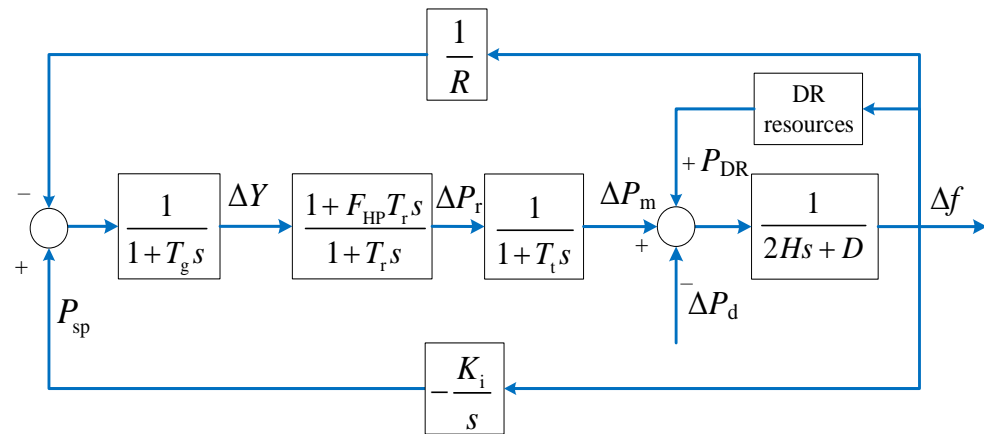


Figure 1. Frequency response model with DR.

The model of the system can be expressed by the state-space equations as follows:

$$\begin{cases} \dot{X} = AX + BP_{DR} + D\Delta P_d \\ Y = CX + v \end{cases} \quad (1)$$

where v is the measurement noise. The matrixes X and Y are the state vector and measurement vector, respectively. A, B, C, D are the coefficient matrixes, which are defined as follows:

$$\begin{aligned} X &= [P_{sp} \quad \Delta Y \quad \Delta P_r \quad \Delta P_m \quad \Delta f]^T \\ A &= \begin{bmatrix} 0 & 0 & 0 & 0 & -K_i \\ \frac{1}{T_g} & -\frac{1}{T_g} & 0 & 0 & -\frac{1}{T_g R} \\ \frac{F_{HP}}{T_g} & \frac{1}{T_r} - \frac{F_{HP}}{T_g} & -\frac{1}{T_r} & 0 & -\frac{F_{HP}}{T_g R} \\ 0 & 0 & \frac{1}{T_t} & -\frac{1}{T_t} & 0 \\ 0 & 0 & 0 & \frac{1}{2H} & -\frac{D}{2H} \end{bmatrix} \\ B &= [0 \quad 0 \quad 0 \quad 0 \quad \frac{1}{2H}]^T \\ C &= [0 \quad 0 \quad 0 \quad 0 \quad 1] \\ D &= [0 \quad 0 \quad 0 \quad 0 \quad -\frac{1}{2H}]^T \end{aligned} \quad (2)$$

The discrete form of the state-space equations can be derived as the following:

$$\begin{cases} X(k) = A_K X(k-1) + B_K P_{DR}(k-1) + D_K \Delta P_d(k-1) \\ Y(k) = C_K X(k) + v(k) \end{cases} \quad (3)$$

where k represents the time step and A_K, B_K, C_K, D_K are the coefficient matrix of the discretized state-space equations. Given the time step size T_{step} , the matrixes can be calculated as follows:

$$\begin{cases} A_K = I + A \cdot T_{step} \\ B_K = B \cdot T_{step} \\ C_K = C \\ D_K = D \cdot T_{step} \end{cases} \quad (4)$$

2.2. Hybrid Hierarchical DR Control Strategy

The structure of hybrid hierarchical DR control is shown in Figure 2, which includes the control center, individual controllers, and ON/OFF appliances. The appliances that are mainly the ON/OFF switching loads include air conditioners, water heaters, and refrigerators. The control commands are calculated in the control center and broadcast to each individual controller. The individual controller measures the frequency of the power system and calculates the specified command to control the ON/OFF status of each appliance.

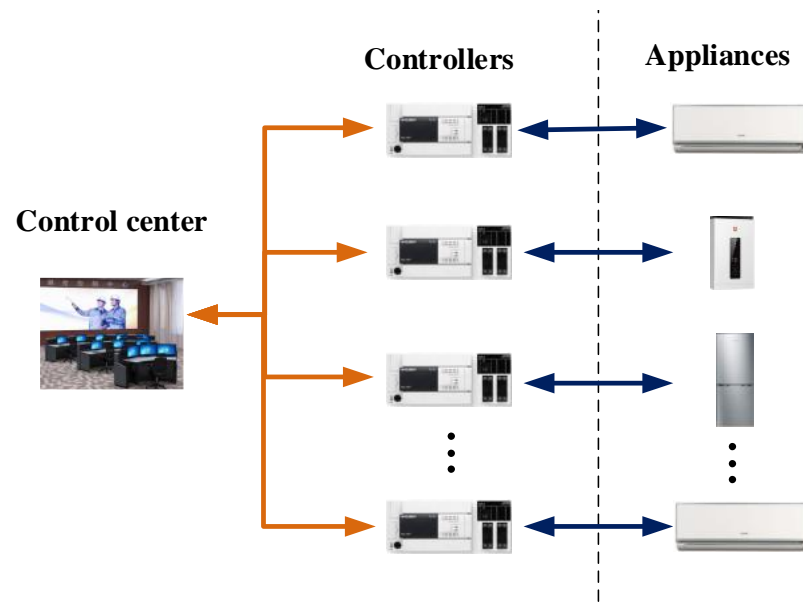


Figure 2. The structure of the hybrid hierarchical DR control.

The appliances can be simplified into ON-appliance and OFF-appliance states according to the switch status. The ON/OFF states of ON- and OFF-appliances should be changed if the frequency deviation occurs. If there is a negative deviation in the system frequency, the ON-appliances should be gradually switched OFF to help raise the system frequency. On the contrary, if there is a positive deviation in the system frequency, the OFF-appliances should be gradually switched ON to help decrease the system frequency. To ensure a smooth adjustment, the power consumption of the ON- and OFF-appliances should be adjusted according to the magnitude of the frequency deviation. The relationship can be expressed as follows:

$$P_{DRoff} = \begin{cases} 0 & \text{if } 0 > \Delta f \geq -\Delta f_{db} \\ -K_{DRoff}(\Delta f + \Delta f_{db}) & \text{if } \Delta f_{prloff} \leq \Delta f \leq -\Delta f_{db} \\ P_{DRmoff} & \text{if } \Delta f \leq \Delta f_{prloff} \end{cases} \quad (5)$$

$$P_{DRon} = \begin{cases} 0 & \text{if } 0 < \Delta f \leq \Delta f_{db} \\ K_{DRon}(\Delta f - \Delta f_{db}) & \text{if } \Delta f_{db} \leq \Delta f \leq \Delta f_{prmon} \\ P_{DRmon} & \text{if } \Delta f \geq \Delta f_{prmon} \end{cases} \quad (6)$$

where P_{DRoff} is the power consumption of the ON-appliances that should be switched off, P_{DRon} is the power consumption of the OFF-appliances that should be switched on, P_{DRmoff} is the capacity (maximum available kW power) of the ON-appliances that can be switched off, P_{DRmon} is the capacity of the OFF-appliances that can be switched on, Δf_{db} is the dead band of the frequency deviation, and Δf_{prloff} and Δf_{prmon} are the minimum frequency deviation and maximum frequency deviation, respectively. The coefficients K_{DRoff} and K_{DRon} are calculated as follows:

$$\begin{cases} K_{DRoff} = \frac{P_{DRmoff}}{(\Delta f_{db} - \Delta f_{prloff})} \\ K_{DRon} = \frac{P_{DRmon}}{(\Delta f_{prmon} - \Delta f_{db})} \end{cases} \quad (7)$$

The responsive appliances in the demand side are ON/OFF loads, which can only be discretely controlled. As shown in Figure 3, the total power consumption of responsive appliances is calculated as follows:

$$P_{DR} = P_{DRoff} - P_{DRon} \quad (8)$$

In addition, the total power consumption is the accumulative sum of the power consumption of each appliance, which can be expressed as the following:

$$\begin{cases} P_{DRoff} = \sum_{i=1}^{n_1} P_{DRoff,i} S_{off,i} \\ P_{DRon} = \sum_{i=1}^{n_2} P_{DRon,i} S_{on,i} \end{cases} \quad (9)$$

where n_1 is the total number of ON-appliances and n_2 is the total number of OFF-appliances; $S_{off,i}$ and $S_{on,i}$ represent the ON/OFF status of ON- and OFF-appliances, respectively. The ON/OFF status can be denoted as a zero-one value, where zero represents the original state and one represents the changed state. For the ON-appliances, $S_{off,i} = 0$ represents the ON state and $S_{off,i} = 1$ represents the OFF state, whereas for the OFF-appliances, $S_{on,i} = 0$ represents the OFF state and $S_{on,i} = 1$ represents the ON state.

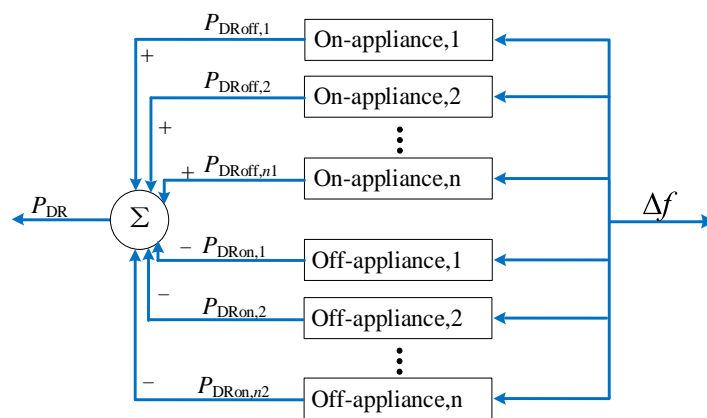


Figure 3. The model of DR resources.

The appliances are sorted with priority. The appliance with the lowest priority responds first. The threshold of the i -th appliance is calculated as follows:

$$\begin{cases} \Delta f_{thoff}(i) = -\Delta f_{db} - \frac{\sum_{k=1}^i P_{DRoff,k}}{K_{DRoff}} \\ \Delta f_{thon}(i) = \Delta f_{db} + \frac{\sum_{k=1}^i P_{DRon,k}}{K_{DRon}} \end{cases} \quad (10)$$

To avoid frequent switching, a delay is set for each appliance. The delay of the i -th appliance is calculated as follows:

$$\begin{cases} T_{off}(i) = T_{off0} + \frac{\sum_{k=1}^i P_{DRoff,k}}{K_{reoff}} \\ T_{on}(i) = T_{on0} + \frac{\sum_{k=1}^i P_{DRon,k}}{K_{reon}} \end{cases} \quad (11)$$

where T_{off0} and T_{on0} are the minimum delays of the firstly switched OFF/ON-responsive appliances and K_{reoff} and K_{reon} are the recovery coefficients.

The control logic of the individual controller is shown in Figure 4. The operation of the individual controller is separated into two branches depending on the value of the frequency deviation. The switching signal to turn on the appliance is generated if the detected frequency deviation is larger than the upper threshold Δf_{thon} (calculated based on (10)). The switching signal to turn off the appliance is generated if the detected frequency deviation is smaller than the lower threshold Δf_{thoff} (calculated based on (10)). The appliance is switched on/off to minimize the frequency deviation. Subsequently, the

delay is initialized when the worst frequency deviation is detected. The delay T_{on} is set when the maximum frequency deviation Δf_{max} is detected. The delay T_{off} is set when the minimal frequency deviation Δf_{min} is detected. The appliances return to their initial status when the delay expires and the frequency deviation is within the allowable range.

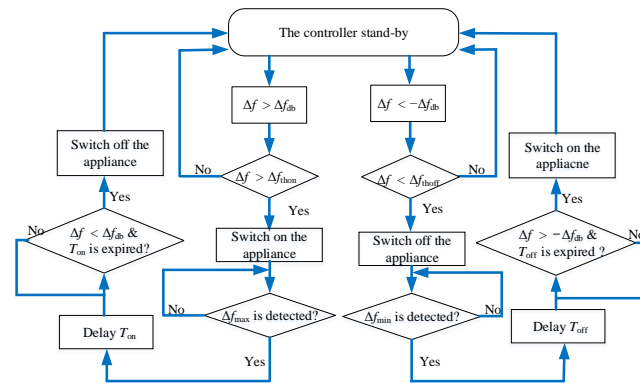


Figure 4. The control logic of the individual controller.

3. The Proposed Method

The system model and DR control strategy have been introduced in the previous section. However, there will always be noise in the frequency detection process, which causes frequency measurement errors and deteriorated frequency control performance. This subsection presents a disturbance estimation-based Kalman filtering method to solve the problem.

3.1. Framework of the Disturbance Estimation-Based Kalman Filtering

The framework of the disturbance estimation-based Kalman filtering is shown in Figure 5.

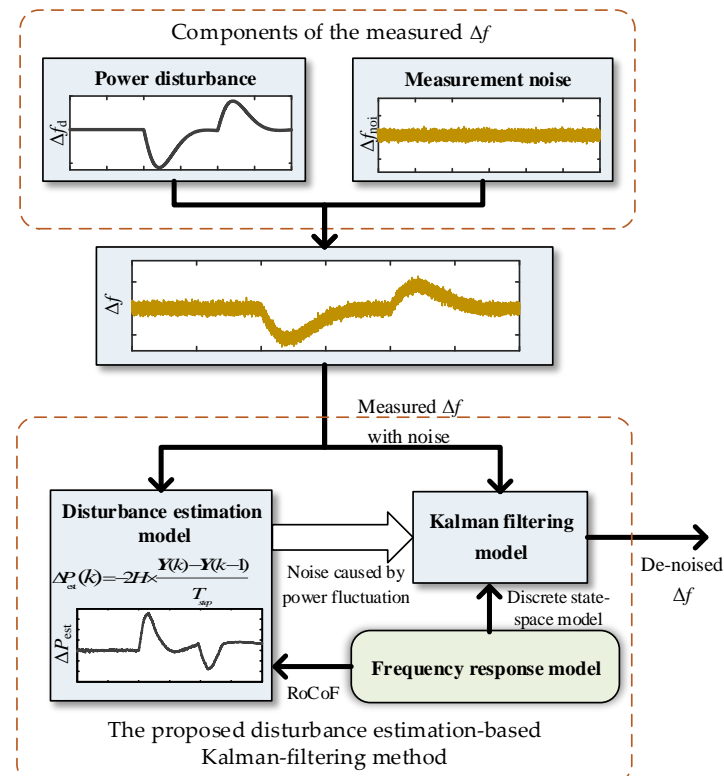


Figure 5. Framework of disturbance estimation-based Kalman filtering.

It can be seen from Figure 5 that the measured frequency Δf includes two components: one is caused by the power disturbance (denoted by ΔP_d), and the other is caused by the measurement noise (denoted by Δf_{noi}). By using the RoCoF derived from the frequency response model, the frequency disturbance ΔP_d caused by the power fluctuation can be separated from the noise. The estimated power ΔP_{est} is taken as the input of the Kalman filter, and the accuracy of the frequency detection can be improved. The de-noised frequency Δf is delivered to the DR controller to improve the frequency control performance.

3.2. Disturbance Estimation

In order to improve the accuracy of frequency detection and enable demand response resources to more accurately participate in system frequency control, it is necessary to estimate the system disturbance based on the RoCoF, which is derived from the system frequency response (SFR) model by which the frequency response can be calculated in closed form. The RoCoF derived from SFR provides a simple but fairly accurate method to estimate the system disturbance [18,19]. The simplified frequency response model is shown in Figure 6.

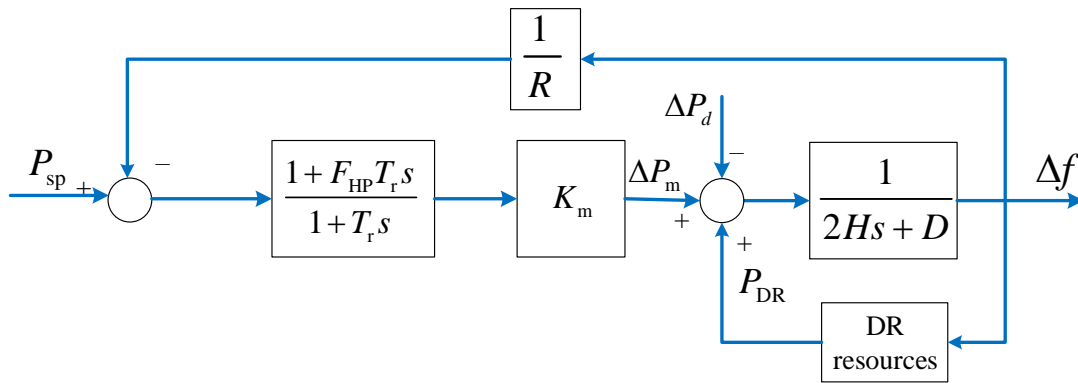


Figure 6. The simplified frequency response model.

By analyzing the block diagram of Figure 6, the frequency deviation Δf can be expressed as follows:

$$\Delta f = \left(\frac{Rf_n^2}{DR + K_m} \right) \left(\frac{K_m(1 + F_{HP}T_r s)P_{sp} - (1 + T_r s)\Delta P_d + (1 + T_r s)P_{DR}}{s^2 + 2\zeta f_n s + f_n^2} \right) \tag{12}$$

where

$$\zeta = \left(\frac{2HR + (DR + K_m F_{HP})T_r}{2(DR + K_m)} \right) f_n \tag{13}$$

and K_m is the generating gain.

In order to investigate the influence of ΔP_d on the system, it is assumed that $P_{sp} = 0$ and $P_{DR} = 0$, then the system is further simplified. Meanwhile, assuming that the system is subjected to a step disturbance denoted as $\Delta P_d(s) = \frac{P_{est}'}{s}$ (with P_{est}' denoting the magnitude of the disturbance); when substituting this expression into (12), Δf can be calculated as follows:

$$\Delta f = \left(\frac{Rf_n^2}{DR + K_m} \right) \left(\frac{(1 + T_r s)P_{est}'}{s(s^2 + 2\zeta f_n s + f_n^2)} \right) \tag{14}$$

Then, the time domain equation can be expressed as the following:

$$\Delta f(t) = \left(\frac{RP_{est}'}{DR + K_m} \right) \left(1 + ae^{-\zeta f_n t} \sin(f_n t + \varphi) \right) \tag{15}$$

where

$$\begin{aligned} f_r &= f_n \sqrt{1-\zeta^2} \\ a &= \sqrt{\frac{1-2T_r\zeta f_n+T_r^2 f_n^2}{1-\zeta^2}} \\ \varphi &= \varphi_1 - \varphi_2 = \tan^{-1}\left(\frac{f_r T_r}{1-\zeta f_n T_r}\right) - \tan^{-1}\left(\frac{\sqrt{1-\zeta^2}}{-\zeta}\right) \end{aligned} \quad (16)$$

The derivative of frequency deviation can be derived by:

$$\frac{d\Delta f(t)}{dt} = \frac{af_n \times R \times P_{est}'}{D \times R \times K_m} \left(e^{-\zeta f_n t} \sin(f_r t + \varphi) \right) \quad (17)$$

At $t = 0$, the maximum rate of frequency deviation Δf can be obtained:

$$\left. \frac{d\Delta f(t)}{dt} \right|_{t=0} = \frac{af_n \times R \times P_{est}'}{D \times R \times K_m} \sin \varphi = \frac{P_{est}'}{2H} \quad (18)$$

The initial slope of frequency deviation can be calculated as follows:

$$m = \left. \frac{d\Delta f(t)}{dt} \right|_{t=0} = \frac{P_{est}'}{2H} \quad (19)$$

Then,

$$P_{est}' = 2H \times m \quad (20)$$

Consequently, the system disturbance estimation can be calculated using the observation vectors $\mathbf{Y}(k)$ and $\mathbf{Y}(k-1)$.

$$\Delta P_{est}(k) = -2H \times \frac{\mathbf{Y}(k) - \mathbf{Y}(k-1)}{T_{step}} \quad (21)$$

3.3. Disturbance Estimation-Based Kalman Filtering

The disturbance estimation-based Kalman filtering can be used to improve the measurement accuracy when the discretized state-space equation of the system is known.

The proposed method can be divided into the time updating equation and measurement updating equation. The time updating equation (i.e., the prediction stage) calculates the prior estimation of the state variables and the prior estimation of the error covariance at the current time according to the state estimation at the previous time; the state of the current time is estimated according to the posterior estimation of the previous time, and the prior estimation of the current time is obtained; the measurement updating equation (i.e., the updating stage) is responsible for combining the prior estimation with the new measurement variables to construct the improved posterior estimation. The time renewal equation and measurement renewal equation are also referred to as the prediction equation and correction equation. The algorithm of disturbance estimation-based Kalman filtering, when applied to frequency detection, is a recursive prediction correction method, including a total of five equations. The process is generally summarized as follows:

$$\hat{\mathbf{X}}_1(k) = \mathbf{A}_K \hat{\mathbf{X}}(k-1) + \mathbf{B}_K \mathbf{P}_{DR}(k-1) + \mathbf{D}_K \Delta P_{est}(k-1) \quad (22)$$

$$\hat{\mathbf{P}}_1(k) = \mathbf{A}_K \hat{\mathbf{P}}(k-1) \mathbf{A}_K^T + \mathbf{Q}_K \quad (23)$$

$$\mathbf{H}(k) = \hat{\mathbf{P}}_1(k) \mathbf{C}_K^T \left(\mathbf{C}_K \hat{\mathbf{P}}_1(k) \mathbf{C}_K^T + \mathbf{R}_K \right)^{-1} \quad (24)$$

$$\hat{\mathbf{X}}(k) = \hat{\mathbf{X}}_1(k) + \mathbf{H}(k) (\mathbf{Y}(k) - \mathbf{C}_K \hat{\mathbf{X}}_1(k)) \quad (25)$$

$$\hat{\mathbf{P}}(k) = (\mathbf{I} - \mathbf{H}(k) \mathbf{C}_K) \hat{\mathbf{P}}_1(k) \quad (26)$$

where A_K , B_K , C_K , D_K , Y , and P_{DR} are defined in Section 2. \hat{X} represents the posterior state estimate, which represents the optimal estimate; \hat{X}_1 is the a priori state estimate, which is the result predicted according to the optimal estimation at the previous time; \hat{P} represents the posterior estimate covariance (The covariance of \hat{X}); \hat{P}_1 is the a priori estimated covariance (The covariance of \hat{X}_1); H is the Kalman gain; Q_K is the covariance matrix of the process noise; and R_K is the covariance matrix of the measurement noise.

4. Results and Discussion

4.1. Performance of Disturbance Estimation

In order to further verify the accuracy of the model for the estimation of the magnitude of system disturbance, the corresponding relative errors were analyzed by considering the estimation of system disturbance at different ΔP_d values, respectively.

As shown in Figure 7, when the system is subjected to different disturbances (ΔP_d), the disturbances can be estimated by using the disturbance estimation model. The statistics are summarized in Table 1. The minimal value of relative error is about 1.8%, and the maximal value of relative error is about 13%. The values of relative error are within 15%. Therefore, the influence of the disturbance can be decreased. The results can be more accurate with the disturbance estimation model.

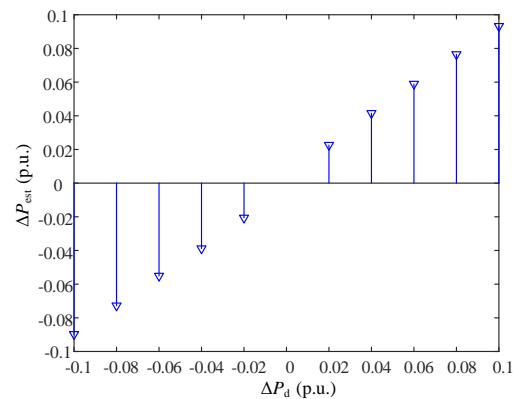


Figure 7. ΔP_{est} values estimated at different ΔP_d values.

Table 1. Disturbance estimation and relative error.

ΔP_d (p.u.)	$\Delta P_{est\ max}$ (p.u.)	Relative Error (%)
-0.1	-0.089	10.266
-0.08	-0.0728	9.0471
-0.06	-0.0551	8.1528
-0.04	-0.0388	2.8796
-0.02	-0.0206	3.0982
0.02	0.0226	13.0230
0.04	0.0415	3.8258
0.06	0.0589	1.7988
0.08	0.0765	4.4022
0.1	0.0932	6.7842

4.2. Performance of Disturbance Estimation-based Kalman Filtering

To verify the effectiveness of the proposed method of disturbance estimation-based Kalman filtering validation in frequency estimation, the performance of the frequency detection is examined without considering the role of DR in the frequency control. The following frequency detection methods are compared:

- (1) Without filter: the frequency is detected without filtering.
- (2) Low-pass filter (LPF): the detected frequency is filtered by an LPF, which is a traditional method of frequency measurement de-noising [20,21].
- (3) Kalman filtering without disturbance estimation: the detected frequency is filtered by Kalman filtering, which follows the idea of [17].
- (4) The proposed disturbance estimation-based Kalman filtering method.

The simulation assumes that the disturbances ($\Delta P_{d1} = 0.1$ p.u., $\Delta P_{d2} = -0.04$ p.u., $\Delta P_{d3} = -0.12$ p.u.) occur at 10 s, 30 s, and 60 s, respectively, considers a nominal frequency of 50 Hz, and considers that Δf_{db} is set to 0.05 Hz. The parameters for the frequency response model are summarized in Table 2.

Table 2. Parameters for the frequency response model.

Parameter	Value
R	0.05
T_g	0.2 s
T_r	7 s
H	5 s
T_t	0.3 s
F_{HP}	0.3
D	1
K_i	1.9

In Figure 8, it can be seen that the method of disturbance estimation-based Kalman filtering results in a more precisely estimated Δf . The root-mean-square deviation (RMSD) and the integral square error (ISE) between the actual frequency deviation Δf and the estimated frequency deviation Δf by the four methods are shown in Figure 8c. The results show that the RMSD and the ISE of disturbance estimation-based Kalman filtering is smaller than the other methods, meaning that the proposed method in this paper can greatly reduce the measurement error and make the detection result more accurate.

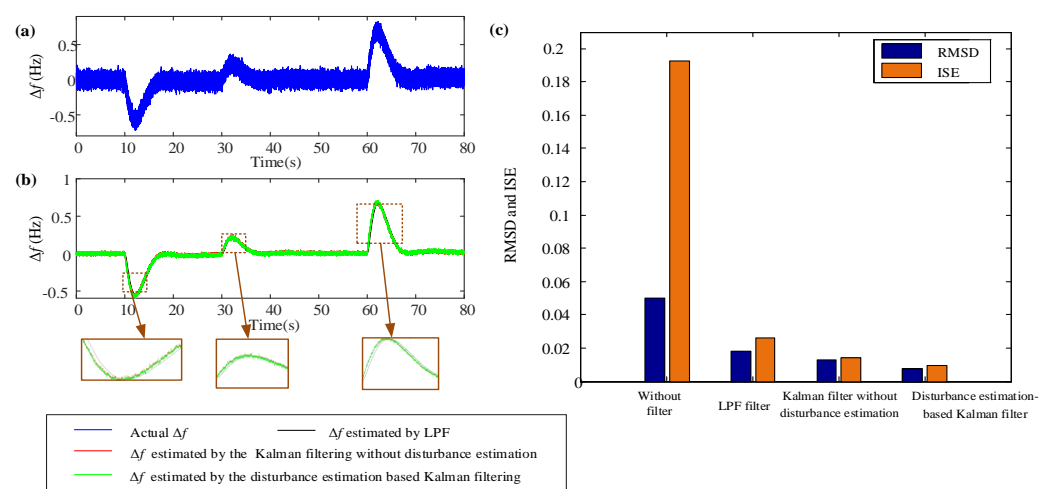


Figure 8. Δf estimated by the four methods: (a) Δf with measurement noise; (b) Δf estimated by the four methods; (c) RMSD and ISE of the four methods.

4.3. Performance of DR in Frequency Control

This subsection investigates the performance of DR in the frequency control. The parameters for DR are summarized in Table 3. The comparison of frequency detection by

different methods are shown in Figure 9. As shown in Figure 9b, the proposed method has a good performance. The maximum value of frequency drop and the maximum value of frequency rise is the smallest using the proposed method. Meanwhile, it is observed that the demand-side appliances are dispatched to participate in the frequency control when the system is subjected to the disturbances, that the potential of DR will decrease, and that the curve of available up/down-regulated DR appliances will rapidly drop. The potential of DR will rise as the frequency recovers, and the method proposed in this paper has a great potential of available DR resources. The results also proves that this method has a good performance in frequency control using DR.

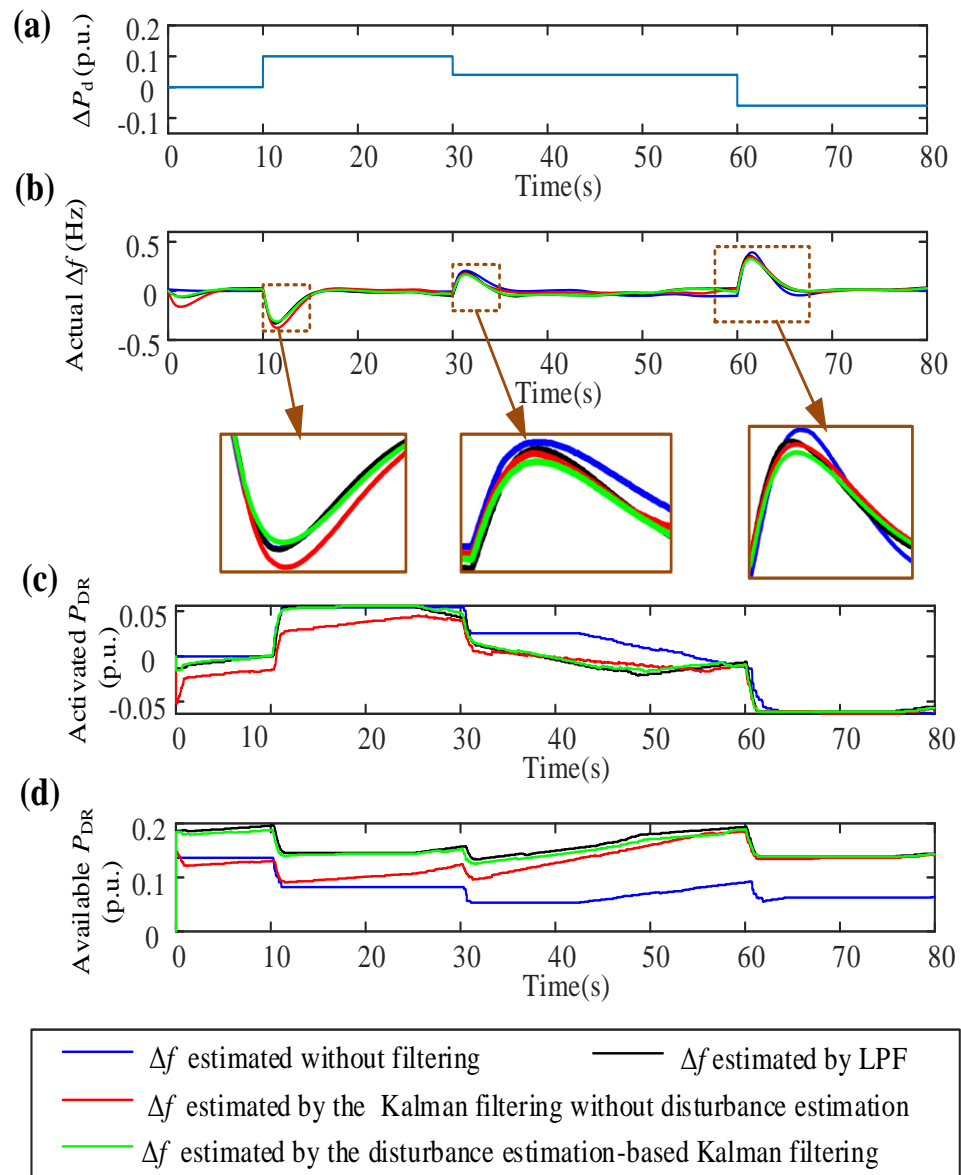


Figure 9. Comparison of frequency detection by different methods: (a) ΔP_d ; (b) actual Δf ; (c) activated DR appliances; (d) available DR appliances.

Table 3. Parameters for DR.

Parameters	Value
K_{reoff}	0.0012 p.u./s
K_{reoon}	0.002 p.u./s
T_{off0}	10 s
T_{on0}	10 s
P_{DRmoff}	0.1 p.u.
P_{DRmon}	0.1 p.u.

The maximum frequency deviation and the maximum activated DR appliances under different ΔP_d values are shown in Figure 10. It can be seen that the absolute value of frequency deviation under different ΔP_d values is smallest by using the proposed method; the DR appliances more precisely respond to the frequency deviation, and the frequency control performance is improved.

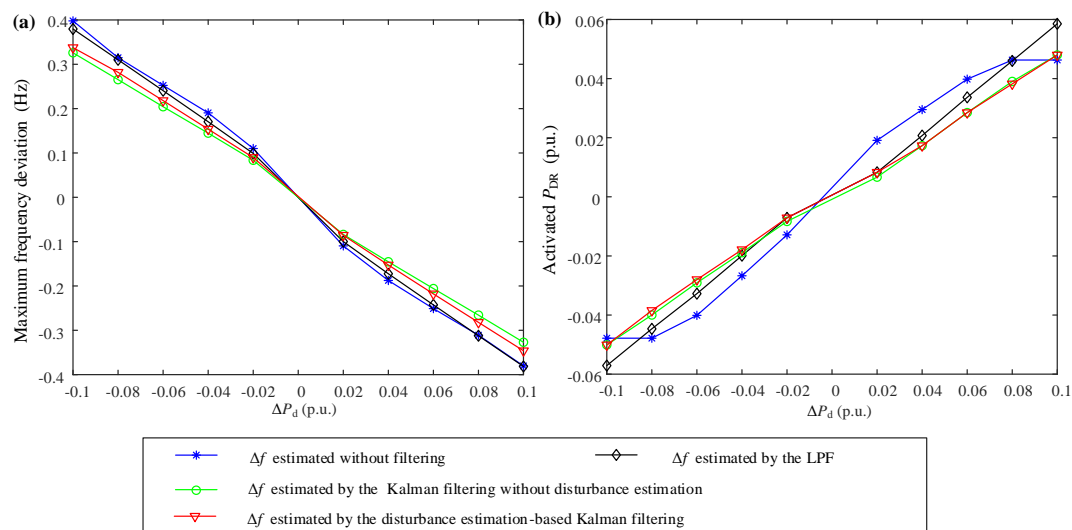


Figure 10. Maximum frequency deviation and maximum activated DR under different ΔP_d values (a) Maximum frequency deviation. (b) Maximum activated DR appliances.

4.4. Discussion

As demonstrated by the simulation results, the proposed disturbance estimation-based Kalman filtering method can help improve the accuracy of the frequency detection and therefore improve the frequency control performance. The results are from three aspects:

- (1) Disturbance estimation: the disturbance estimation model can accurately estimate the step disturbance with a low relative error.
- (2) Frequency detection: the Kalman filtering with the above-mentioned disturbance estimation model can more accurately measure the system frequency than traditional methods.
- (3) Frequency control: the DR control strategy with the above-mentioned frequency detection method results in a better frequency control performance.

5. Conclusions

In this paper, DR using a disturbance estimation-based Kalman filtering method was proposed for frequency control. The main work of this paper included the following:

- (1) The disturbance estimation-based Kalman filtering method was developed to improve the accuracy of frequency detection.

- (2) The proposed Kalman filtering method was applied to the DR to improve the frequency control performance.

We conclude that the proposed method can more accurately detect the system frequency and make the demand response more accurately participate in the frequency control. Future work may be aimed at designing hardware controllers that can put into practice the disturbance estimation Kalman filtering in frequency control applications with DR.

Author Contributions: Conceptualization, X.W., Q.Q. and Y.B.; methodology, X.W., Q.Q. and Y.B.; validation, X.W., Q.Q. and Y.B.; formal analysis, X.W., Q.Q. and Y.B.; investigation, Q.Q.; resources, Y.B.; data curation, Q.Q.; writing—original draft preparation, Q.Q.; writing—review and editing, X.W.; visualization, X.W.; supervision, Y.B.; project administration, Y.B.; funding acquisition, Y.B. All authors have read and agreed to the published version of the manuscript.

Funding: This research was funded by the National Natural Science Foundation of China (51707099).

Data Availability Statement: Not applicable.

Acknowledgments: The authors would like to express their gratitude for the valuable recommendations made by the reviewers to improve the quality of this paper.

Conflicts of Interest: The authors declare no conflict of interest.

References

- Martinez-Rico, J.; Zulueta, E.; de Argandoña, I.R.; Fernandez-Gamiz, U.; Armendia, M. Multi-objective optimization of production scheduling using particle swarm optimization algorithm for hybrid renewable power plants with battery energy storage system. *J. Mod. Power Syst. Clean Energy* **2021**, *9*, 285–294. [[CrossRef](#)]
- Chen, C.; Bao, Y.Q.; Wu, X.H.; Wang, B. Incremental Cost Consensus Algorithm for On/Off Loads to Enhance the Frequency Response of the Power System. *IEEE Access* **2020**, *8*, 67687–67697. [[CrossRef](#)]
- He, S.; Gao, H.; Tian, H.; Wang, L.; Liu, Y.; Liu, J. A two-stage robust optimal allocation model of distributed generation considering capacity curve and real-time price based demand response. *J. Mod. Power Syst. Clean Energy* **2021**, *9*, 114–127. [[CrossRef](#)]
- Zaman, M.S.U.; Bukhari, S.B.A.; Hazazi, K.M.; Haider, Z.M.; Haider, R.; Kim, C.-H. Frequency Response Analysis of a Single-Area Power System with a Modified LFC Model Considering Demand Response and Virtual Inertia. *Energies* **2018**, *11*, 787. [[CrossRef](#)]
- Patil, S.; Deshmukh, S.R. Development of Control Strategy to Demonstrate Load Priority System for Demand Response Program. In Proceedings of the 2019 IEEE International WIE Conference on Electrical and Computer Engineering (WIECON-ECE), Bangalore, India, 15–16 November 2019. [[CrossRef](#)]
- Molina-Garcia, A.; Bouffard, F.; Kirschen, D.S. Decentralized Demand-Side Contribution to Primary Frequency Control. *IEEE Trans. Power Syst.* **2011**, *26*, 411–419. [[CrossRef](#)]
- Nandkeolyar, S.; Mohanty, R.K.; Dash, V.A. Management of time-flexible demand to provide power system frequency response. In Proceedings of the International Conference on Technologies for Smart City Energy Security and Power: Smart Solutions for Smart Cities, Bhubaneswar, India, 28–30 March 2018; pp. 1–4.
- Gong, F.; Han, N.; Zhang, L.; Ruan, W. Analysis of Electricity Consumption Behavior of Air Conditioning based on the Perspective of Power Demand Response. In Proceedings of the 2020 IEEE International Conference on Advances in Electrical Engineering and Computer Applications (AEECA). *IEEE* **2020**, *8*, 412–416.
- Bao, Y.Q.; Li, Y.; Hong, Y.Y.; Wang, B. Design of a Hybrid Hierarchical Demand Respond Control Scheme for the Frequency Control. *IET Gener. Transm. Distrib.* **2015**, *9*, 2303–2310. [[CrossRef](#)]
- Shen, Y.; Li, Y.; Zhang, Q.; Li, F.; Wang, Z. Consumer psychology based optimal portfolio design for demand response aggregators. *J. Mod. Power Syst. Clean Energy* **2021**, *9*, 431–439. [[CrossRef](#)]
- Hu, Y.; Liu, J.; Xu, X. Dynamic Interactions between Local Energy Systems Coupled by Power and Gas Distribution Networks. *Energies* **2022**, *15*, 8420. [[CrossRef](#)]
- Li, M.; Ye, J. Design and Implementation of Demand Side Response Based on Binomial Distribution. *Energies* **2022**, *15*, 8431. [[CrossRef](#)]
- Dash, P.K.; Pradhan, A.K.; Panda, G. Frequency estimation of distorted power system signals using extended complex Kalman filter. *IEEE Trans. Power Deliv.* **1999**, *14*, 761–766. [[CrossRef](#)]
- Huang, C.-H.; Lee, C.-H.; Shih, K.-J.; Wang, Y.-J. Frequency Estimation of Distorted Power System Signals Using Robust Extended Complex Kalman Filter. In Proceedings of the Intelligent Systems Applications to Power Systems, Kaohsiung, Taiwan, 5–8 November 2007.
- Kanna, S.; Dini, D.H.; Xia, Y.; Hui, S.Y.; Mandic, D.P. Distributed Widely Linear Kalman Filtering for Frequency Estimation in Power Networks. *IEEE Trans. Signal Inf. Process. Over Netw.* **2015**, *1*, 45–57. [[CrossRef](#)]

16. Mathieu, J.L.; Koch, S.; Callaway, D.S. State Estimation and Control of Electric Loads to Manage Real-Time Energy Imbalance. *IEEE Trans. Power Syst.* **2013**, *28*, 430–440. [[CrossRef](#)]
17. Bao, Y.-Q.; Shen, C.; Wang, Q.; Zhang, J.-L. Demand Response Based on Kalman Filtering for the Frequency Control. *J. Electr. Eng. Technol.* **2019**, *14*, 1087–1094. [[CrossRef](#)]
18. Chang-Chien, L.-R.; An, L.N.; Lin, T.-W.; Lee, W.-J. Incorporating Demand Response with Spinning Reserve to Realize an Adaptive Frequency Restoration Plan for System Contingencies. *IEEE Trans. Smart Grid* **2012**, *3*, 1145–1153. [[CrossRef](#)]
19. Anderson, P.M.; Mirhey, D.R.M. A low-order system frequency response model. *IEEE Trans. Power Syst.* **2002**, *5*, 720–729. [[CrossRef](#)]
20. Zhou, W.; Mu, L.; Rui, Y. A Frequency Detection Algorithm Based on dq Coordinate Transformation. In Proceedings of the 2010 Asia-Pacific Power and Energy Engineering Conference, Chengdu, China, 28–31 March 2010; pp. 1–4.
21. Li, Q.; Wang, W.; Qin, L.; Zou, L.; Li, Q. Investigation on a methodology to detect instantaneous reactive and harmonic currents in single-phase systems. In Proceedings of the 2008 International Conference on Electrical Machines and Systems, Wuhan, China, 17–20 October 2008; pp. 3887–3891.